eNeuro Accepted Manuscript

eNeuro

Research Article: New Research | Disorders of the Nervous System

Altered cerebellar response to somatosensory stimuli in the *Cntnap2* mouse model of autism

https://doi.org/10.1523/ENEURO.0333-21.2021

Cite as: eNeuro 2021; 10.1523/ENEURO.0333-21.2021

Received: 12 August 2021
Revised: 1 September 2021
Accepted: 13 September 2021

This Early Release article has been peer-reviewed and accepted, but has not been through the composition and copyediting processes. The final version may differ slightly in style or formatting and will contain links to any extended data.

Alerts: Sign up at www.eneuro.org/alerts to receive customized email alerts when the fully formatted version of this article is published.

Copyright © 2021 Fernández et al.
This is an open-access article distributed under the terms of the Creative Commons Attribution 4.0 International license, which permits unrestricted use, distribution and reproduction in any medium provided that the original work is properly attributed.

eNeuro Accepted Manuscript

Title page

1.-Manuscript Title (50 word maximum)

Altered cerebellar response to somatosensory stimuli in the *Cntnap2* mouse model of autism

2. Abbreviated Title (50 character maximum)

3. List all Author Names and Affiliations in order as they would appear in the published article

Marta Fernández, Department of Pharmacology, University of the Basque Country UPV/EHU, Leioa 48940, Spain
Carlos A. Sánchez-León, Department of Physiology, Anatomy and Cellular Biology, Pablo de Olavide University, Seville 41013, Spain. Leibniz Research Center for Working Environment and Human Factors, Department of Psychology and Neurosciences, TU Dortmund, Dortmund, Germany
Javier Llorente, Department of Pharmacology, University of the Basque Country UPV/EHU, Leioa 48940, Spain
Teresa Sierra-Arregui, Department of Pharmacology, University of the Basque Country UPV/EHU, Leioa 48940, Spain
Shira Knafo, Department of Physiology and Cell Biology, The National Institute for Biotechnology in the Negev, and The Zlotowski Center for Neuroscience, Ben-Gurion University of the Negev, Beer-Sheva, Israel. Ikerbasque, Basque Foundation for Science and Instituto Biofisika (UPV/EHU, CSIC), Leioa E-48940, Spain
Javier Márquez-Ruiz, Department of Physiology, Anatomy and Cellular Biology, Pablo de Olavide University, Seville 41013, Spain.
Olga Peñagarikano, Department of Pharmacology, University of the Basque Country UPV/EHU, Leioa 48940, Spain. Centro de Investigación Biomédica en Red de Salud Mental (CIBERSAM), 48940 Leioa, Spain

4. Author Contributions:

SK, JMR and OP designed research, MF, CASL, JL and TSA performed research and analyzed data. All authors contributed to writing the paper.

5. Correspondence should be addressed to (include email address)

Marta Fernández, marta.fernandez@ehu.eus
Javier Llorente, javier.llorente@ehu.eus

6. Number of Figures: 4
7. Number of Tables: 0
8. Number of Multimedia: 0
9. Number of words for Abstract: 208
10. Number of words for Significance Statement: 159
11. Number of words for Introduction: 403
12. Number of words for Discussion: 813

13. Acknowledgements

The authors thank the SGIker Microscopy Core (UPV/EHU, ERDF, ESF) for technical support and Drs. Jorge Valero and Jan Tønnesen, from Achucarro Basque Center for Neuroscience, for help with neuroanatomical analyses. This work was supported by MCIU/AEI/FEDER, UE grant RTI2018-101427-B-I00 to OP, ERANET-NEURON grant nEUrotalk to OP and UPV/EHU grant GIU18/094 to OP; Israel Science Foundation (536/19) to SK; Spanish Ministry of Science (Europa Excelencia 15/02, SAF2016-78071-R to SK; BFU2017-89615-P from the Spanish MINECO-FEDER to JMR. MF

eNeuro Accepted Manuscript

holds a MINECO predoctoral fellowship (BES-2016-078420) and TS-A is a Basque Government predoctoral fellow (PRE-2020-2-0109).

14. Conflict of Interest

Authors report no conflict of interest

15. Funding sources

Funding agency	Reference	PI
MCIU/AEI/FEDER, UE	RTI2018-101427-B-I00	OP
ERANET-NEURON	nEUrotalk	OP
UPV/EHU	GIU18/094	OP
Israel Science Foundation	(536/19)	SK
MCIU	SAF2016-78071-R	SK
MINECO-FEDER	BFU2017-89615-P	JMR.
MINECO predoctoral fellowship	BES-2016-078420	MF
Basque Government predoc fellowship (PRE-2020-2-0109)		TS-A

eNeuro Accepted Manuscript

Altered cerebellar response to somatosensory stimuli in the *Cntnap2* mouse model of autism

Marta Fernández[1*], Carlos A. Sánchez-León[2,3], Javier Llorente[1*], Teresa Sierra-Arregui[1], Shira Knafo[4], Javier Márquez-Ruiz[2], Olga Peñagarikano[1,5]

[1]Department of Pharmacology, University of the Basque Country UPV/EHU, Leioa 48940, Spain

[2]Department of Physiology, Anatomy and Cellular Biology, Pablo de Olavide University, Seville 41013, Spain

[3]Leibniz Research Center for Working Environment and Human Factors, Department of Psychology and Neurosciences, TU Dortmund, Dortmund, Germany

[4]Department of Physiology and Cell Biology, The National Institute for Biotechnology in the Negev, and The Zlotowski Center for Neuroscience, Ben-Gurion University of the Negev, Beer-Sheva, Israel. Ikerbasque, Basque Foundation for Science and Instituto Biofisika (UPV/EHU, CSIC), Leioa E-48940, Spain

[5]Centro de Investigación Biomédica en Red de Salud Mental (CIBERSAM), 48940 Leioa, Spain

*For correspondence: marta.fernandez@ehu.eus; javier.llorente@ehu.eus

Abstract

Atypical sensory processing is currently included within the diagnostic criteria of autism. The cerebellum is known to integrate sensory inputs of different modalities through its connectivity to the cerebral cortex. Interestingly, cerebellar malformations are among the most replicated features found in postmortem brain of individuals with autism. We studied sensory processing in the cerebellum in a mouse model of autism, knockout for the *Cntnap2* gene. *Cntnap2* is widely expressed in Purkinje cells and has been recently reported to regulate their morphology. Further, individuals with *CNTNAP2* mutations display cerebellar malformations and CNTNAP2 antibodies are associated with a mild form of cerebellar ataxia. Previous studies in the *Cntnap2* mouse model show an altered cerebellar sensory learning. However, a physiological analysis of cerebellar function has not been performed yet. We studied sensory evoked potentials in cerebellar Crus I/II region upon electrical stimulation of the whisker pad in alert mice and found striking differences between WT and *Cntnap2* KO mice. In addition, single-cell recordings identified alterations in both sensory-evoked and spontaneous firing patterns of Purkinje cells. These changes were accompanied by altered intrinsic properties and morphological features of these neurons. Together, these results indicate that the *Cntnap2* mouse model could provide novel insight into the pathophysiological mechanisms of autism core sensory deficits.

eNeuro Accepted Manuscript

Significance Statement

Atypical sensory processing is currently included within the diagnostic criteria of autism. The cerebellum is known to integrate sensory inputs of different modalities through its connectivity to the cerebral cortex. In support of this, cerebellar malformations are among the most replicated features found in postmortem brain of individuals with autism. One autism-linked gene associated to cerebellar dysfunction both in humans and animal models is CNTNAP2. In this work, we studied cerebellar integration of sensory information in the Cntnap2 mouse model of autism. We found striking differences between WT and Cntnap2 KO mice that indicate an altered cerebro-cerebellar connection. In addition, single-cell recordings identified alterations in both sensory-evoked and spontaneous firing patterns of Purkinje cells. These alterations were accompanied by altered intrinsic properties and morphological features of these neurons. Although the mechanism of such deficits is not revealed, these data indicate that the Cntnap2 mouse model could be very valuable to identify the pathophysiological mechanisms of ASD core sensory deficits.

eNeuro Accepted Manuscript

Introduction

Atypical sensory processing is currently included within the diagnostic criteria of autism spectrum disorder (ASD) (APA, 2013). The cerebellum is known to play a role in integration of different sensory modalities (e.g. hearing, sight, touch and smell) through its connectivity to the cerebral cortex (Proville et al., 2014). Interestingly, cerebellar malformations are among the most replicated features found in postmortem brain of individuals with autism (Wang et al., 2014) and alterations in functional connectivity between the cerebellum and cortical sensory areas have been found through fMRI (Lidstone et al., 2021).

Loss of function mutations in the *CNTNAP2* gene are associated with a syndromic form of autism that presents with cerebellar abnormalities, including hypoplasia of the cerebellar vermis and hemispheres (Rodenas-Cuadrado et al., 2016). Further, autism-linked common genetic variation in *CNTNAP2* has been associated with reduction in cerebellar grey matter volume, as determined by MRI (Tan et al., 2010). Incidentally, CNTNAP2 antibodies have been identified in sera from patients with otherwise unexplained progressive cerebellar ataxia with mild to severe cerebellar atrophy (Becker et al., 2012; Melzer et al., 2012), supporting the role of this gene in cerebellar development and function. *CNTNAP2* is widely expressed in the cerebellum (Gordon et al., 2016), and it has been recently reported to regulate Purkinje cell (PC) morphology (Argent et al., 2020). In mice, loss of *Cntnap2* function causes autism-like behaviors (Penagarikano et al., 2011), as well as several sensory abnormalities such as hypersensitivity to painful stimuli (Dawes et al., 2018) and alterations in auditory (Scott et al., 2018) as well as olfactory behaviors (Gordon et al., 2016). Neuroanatomical analysis of this model shows an alteration in cerebellar volume, as measured by structural MRI (Ellegood and Crawley, 2015). Classical tests measuring cerebellar function report improved performance in the accelerating rotarod (Penagarikano et al., 2011), unstable gait (Argent et al., 2020) and cerebellar sensory learning defects (Kloth et al., 2015). However, a physiological analysis of cerebellar function has not been performed yet. In this work, we studied sensory processing in the cerebellum in alert *Cntnap2* mice. We discovered alterations in the firing patterns of PC both spontaneous as well as in the evoked response to sensory stimuli. This alteration was accompanied by an increased excitability of PC and reduced dendritic complexity in these neurons. Together, these results

eNeuro Accepted Manuscript

provide novel insight into the pathophysiological mechanisms by which CNTNAP2 mutations cause impairments in cerebellar function that may contribute to ASD core deficits.

Materials and methods

Animals

Adult (8-10 weeks) male mutant mice lacking the *Cntnap2* gene (Cntnap2-KO) and age-matched wild-type controls (C57BL/6 background) were purchased from The Jackson Laboratory (Bar Harbor, ME, USA). Animals were housed 4-5 per cage on a 12-12 h light/dark cycle, at 21-23°C and 65-70% humidity. Food and water were provided *ad libitum*. Animal maintenance and experimental procedures were executed following the guidelines of animal care established by the European Communities Council Directive 2010/63/EU, as well as in agreement with the Spanish Legislation (Royal Decree 53/2013). Procedures were also approved by the Ethics Committee for Animal Welfare (CEBA) of the University of the Basque Country (UPV/EHU) and the Pablo de Olavide University (UPO).

In vivo electrophysiology

We followed the procedures described in Sánchez-León et al. (Sanchez-Leon et al., 2021). Briefly, stereotaxic surgery was performed to open a craniotomy (2mm ø) following the Allen Brain Atlas coordinates for the right Crus I/II area (AP: -6,6 mm; and L: -2,6 mm, relative to Bregma). During surgery, two small bolts were cemented in the skull to immobilize the head during the recording sessions, and a silver reference electrode was placed on the surface of the parietal cortex. The surface of the craniotomy was protected with bone wax (Ethicon, Johnson & Johnson) until recording sessions. After the surgery, mice were allowed to recover for at least two days. For *in vivo* recordings, the animal's head was fixed to the recording setup, consisting of a treadmill with an infrared sensor for monitoring locomotor activity. All experiments were carried out with an amplifier (BVC-700A, Dagan corporation, MN, USA) connected to a dual extracellular-intracellular headstage (8024 Dual Intracellular & Extracellular Headstage, MN, USA). For SEP recordings we used a micropipette with a tip diameter between 8-10 µm, subsequently the pipette was filled with 3 M NaCl and placed on a micromanipulator (Narishige MO-10, Japan). Whisker stimulation was performed with a pair of flexible steel electrodes (Strand ø: 50.8 µm; Coated ø: 228.6 µm; Multi-Stranded PFA-Coated Stainless Steel Wire, A-M

eNeuro Accepted Manuscript

Systems, WA, USA) inserter under the skin of the right whisker pad. The electrical stimulus consisted of a single square pulse (0.2 ms; 0.5-1 mA) delivered by an isolation unit (Cibertec ISU 210 BIP) connected to a stimulator device (CS420, Cibertec), applied every 10±2 s. For single-Purkinje cell activity, a micropipette with a tip diameter around 1-2 µm was filled with 3 M NaCl and placed on a micromanipulator (Narishige MO-10, Japan). The pipette was inserted in the area of interest at ~2 µm/s and spikes were detected based on visual (2002C and 2004C, Tektronix, OR., USA) and auditory cues (Audio monitor 3300, A-M Systems, WA., USA).

Data were collected with a CED micro1401-3 data acquisition unit and sampled at 25 kHz. SEP analysis was performed with EEGLAB rev.14.1.2 toolbox using the Matlab 2015a software package. Recorded data were segmented into 70 ms windows using the electrical stimulation as trigger and baseline was corrected by subtracting the mean voltage level in the first 20 ms interval of the window (before whisker stimulus). Data were averaged for each genotype to obtain the average SEP and temporal periods were statistically compared. For single-cell recording analysis, only well isolated neurons recorded during at least 100s were considered. A DC remove process (time constant (s): 0,001-0,0004) was applied to reduce DC level drifts, and spikes were detected based on threshold-crossing algorithm of Spike2 software. All spikes were visually confirmed and Purkinje cells were identified by the presence of CS. Subsequently, SS and CS of each neuron were analyzed using a Matlab custom-made script. The Predominant Firing Rate represent the mode of the firing rate, the Frequency of the firing rate that appears most often. The Coefficient of variation CV and CV2, as a measure of firing regularity, were calculated following the formulas described in Holt et al. (Holt et al., 1996) $CV=\frac{\sigma ISI}{\mu ISI}$, where ISI represents the inter-spike interval. $CV2=\frac{2|ISI_{n+1}-ISI_n|}{(ISI_{n+1}+ISI_n)}$. The Complex Spikes were sorted manually offline for the duration of the recording.

***Ex vivo* electrophysiology**

Mice were anesthetized with isoflurane and decapitated. The brain was rapidly submerged in ice-cold cutting solution containing (in mM): 20 NaCl, 2.5 KCl, 0.5 $CaCl_2$, 7 $MgCl_2$, 1.25 NaH_2PO_4, 85 sucrose, 25 D-glucose and 60 $NaHCO_3$, saturated with 95% O_2/5% CO_2 (carbogen). The cerebellum was separated from the rest of the brain and the right part cut and glued to the

eNeuro Accepted Manuscript

cutting-dish. Parasagittal slices (250 µm thick) containing the Crus I area were prepared using a Campden Ci 7000smz-2 vibroslicer. Immediately upon cutting, slices were submerged in an artificial cerebrospinal fluid (aCSF) containing (in mM): 126 NaCl, 2.5 KCl, 1.2 $MgCl_2$, 2.4 $CaCl_2$, 1.2 NaH_2PO_4, 11.1 D-glucose, 21.4 $NaHCO_3$, 0.1 ascorbic acid and 0.4 kynurenic acid, bubbled with carbogen at room temperature (22-24 °C), and left to recover for at least 1 h. Slices were constantly perfused with aCSF at 33°C. PCs were visualized using infrared differential interference contrast light (Olympus BX52WI). Patch pipettes pulled from thin borosilicate capillary glass (World Precision Instruments) with a Sutter P-97 horizontal puller had a resistance of 3–5 MΩ. Internal solution contained (in mM): 115 K-gluconate, 10 HEPES, 11 EGTA, 2 $MgCl_2$, 10 NaCl, 2 MgATP, 0.25 Na_2GTP and biocytin (5 mg/ml, B4261 Sigma-Aldrich), pH 7.3, adjusted with NaOH; osmolality ± 275 mOsm.

Intrinsic properties were studied in whole-cell voltage-clamp and in current-clamp mode by injecting a hyperpolarizing bias current (less than -500 pA) to hold membrane potential between -60 and -65 mV and keep the neuron silenced during the rheobase study. Membrane potentials were not corrected for the liquid junction potential between intra and external solution (-12.7 mV). Neurons in which holding current was greater than -500 pA and experiments in which access resistance was higher than 16 MΩ were discarded and not included for analysis. Signals from the patch pipette were recorded with a MultiClamp 700B amplifier, digitized at 10–20 kHz and low-pass filtered at 2–5 kHz with a Digidata 1440A analog-to-digital converter and analyzed off-line using Clampfit 10.7 software (Molecular Devices). Intrinsic excitability was determined in response to increasing depolarizing current pulses (+75 pA) of 750 ms duration injected from hyperpolarized holding currents. Rheobase was registered for each neuron as the net depolarizing current capable of inducing the first action potential (AP). PCs have been described to have different integrative properties making that neurons with similar resistances tend to respond with different firing frequencies to current pulses of similar amplitude and duration (Llinas and Sugimori, 1980). In order to facilitate the comparison between firing frequency curves, rheobase was normalized to zero and only the instantaneous frequencies between the first six APs were analyzed. AP threshold for each neuron was calculated for the first spike as the voltage where dV/dt reaches 5% of the AP maximal rise slope.

eNeuro Accepted Manuscript

Neuroanatomy

PCs were filled during patch-clamp recordings with biocytin (Sigma) via passive diffusion. Filled slices were fixed in 4% paraformaldehyde in PBS for 24h at 4ºC and incubated with Alexa 555/488-Streptavidin (1/500) for 48h at 4ºC. Subsequently the slices were washed with PBS and mounted using Prolong Antifade Gold mounting medium (Invitrogen).

Super-resolution images were acquired using a confocal LSM880 Fast Airyscan microscope using a 25x/0.8 water (for dendrite analysis) and a 63x/0.4 oil (voxel size 49 x 49 x 211 nm, for spine analysis) Plan-Apochromat objectives. Sholl analysis and spine quantification were performed using Fiji imageJ software. For Sholl, the number of intersections of the dendritic arbour with concentric circles drawn at 5 µm intervals from the soma was counted. Spines were manually counted along a 10 µm distal dendrite.

Statistical analysis

Data are displayed through the graphs as mean ± S.E.M. Statistical analyses were performed using Matlab (Math Works Inc.) and Prism (GraphPad). For comparisons between groups a Student's *t* test or two-way ANOVA with repeated measures, when appropriate, were used, as indicated in each figure legend. The significance threshold was set at P=0.05 (ns=not significant, *P<0.05, **P<0.01, ***P<0.001). Effect sizes as denoted by mean differences (MD) are displayed on the right of the graphs, when appropriate. Estimation statistics based on 95% confidence interval (CI) of the mean difference is shown. Plots were performed with https://www.estimationstats.com. Artistic figures were created with Biorender.

Results

Spontaneous *in vivo* Purkinje cell activity is altered in *Cntnap2*$^{-/-}$ mice

We first performed extracellular recordings of spontaneous PC activity in the Crus I/II area of awake animals (**Figure 1A**). Crus I/II was selected because of its functional relationship with sensory whisker inputs (Gao et al., 1996) and its association with autism (Skefos et al., 2014; D'Mello et al., 2016; Wang et al., 2020). PC present two types of firing patterns: simple spikes

eNeuro Accepted Manuscript

(SS) and complex spikes (CS), generated by distinct inputs (parallel fibers and climbing fibers, respectively) and distinguished by their particular waveforms. Despite their different origin interactions between the two types of spikes have been described, such that CS firing is thought to modulate SS activity (Tang et al., 2017). We found a lower CS firing frequency in *Cntnap2* KO mice compared with WT controls (**Figure 1B**). The firing frequency of SS (**Figure 1C**), as well as the predominant, or preferred, SS firing frequency (**Figure 1D**) were not different between genotypes. However, *Cntnap2* KO mice show a higher irregularity in the temporal firing pattern of SS (**Figure 1E**), as measured by the coefficient of variation (CV) of the inter-spike intervals. Such difference is not observed when adjacent inter-spike intervals of presumably burst firing are considered, denoted by CV_2 (**Figure 1F**).

Figure 1. *Cntnap2* mice show altered *in vivo* spontaneous activity of Purkinje cells. (A) Schematic illustration of an extracellular PC recording and a representative trace displaying simple spikes (SS) and complex spikes (CS). (B) CS firing rate, MD -0.259 [95.0% CI -0.426, -0.0951], Student's *t* test *P*=0.0054. (C) SS firing rate, MD 3.68 [95% CI -8.55, 19.0], Student's *t* test *P*=0.656. (D) SS predominant firing rate, MD 14.7 [95.0% CI -15.4, 37.9], Student's *t* test *P*=0.31. (E) Coefficient of variation (CV) of the inter-spike intervals for SS, MD 0.138 [95.0% CI 0.0422, 0.266], Student's *t* test *P*=0.0242. (F) Coefficient of variation for adjacent inter-spike intervals (CV2), MD 0.0439 [95.0% CI -0.0117, 0.103], Student's *t* test *P*=0.153. Data are presented as mean ± S.E.M. N=14 WT, 15 KO neurons. MD= mean difference (KO-WT); CI, confidence interval. **P*<0.05, ***P*<0.01.

eNeuro Accepted Manuscript

Purkinje cell responses to sensory-evoked stimuli are altered in *Cntnap2*$^{-/-}$ mice

To characterize PC activity in response to somatosensory stimuli, we recorded the Local Field Potential (LFP) near the PC layer from the cerebellar Crus I/II area after subcutaneous electrical stimulation of the ipsilateral whisker pad in alert mice (**Figure 2A**).This protocol induces a similar but more reproducible response than tactile whisker stimulation (Marquez-Ruiz and Cheron, 2012).

Concordant with what was previously described (Marquez-Ruiz and Cheron, 2012), in wild-type (WT) mice this electrical stimulation evoked a highly reproducible sensory evoked potential (SEP) with two main negative components appearing at around 4 and 12 ms (3.94±0.13 ms and 12.87±0.40 ms), corresponding to trigeminal (T) and cortical (C) pathways, respectively. Strikingly, the waveform of SEP in *Cntnap2* knockout (KO) mice was notably different, showing the expected T wave (4.10±0.15 ms) and a novel negative peak at around 6ms (6.46±0.14 ms) in the absence of the expected C wave at 12 ms (**Figure 2 B**). To determine the basis for the altered SEP response observed in *Cntnap2*$^{-/-}$ mice, we then recorded unitary PC upon whisker stimulation. Previous studies have correlated the appearance of a SS burst with the above-mentioned T component, whereas CS occurred at post-stimulation latencies concordant with the C component (Mostofi et al., 2010; Marquez-Ruiz and Cheron, 2012). In agreement with this, we found that the probability for a CS to fire around 13 ms (12.87ms) after the stimulus onset in WT mice is coincident with the C wave observed in the SEP. In *Cntnap2*$^{-/-}$ mice, however, the bigger probability for a CS to appear takes place at 6.46 ms, matching the latency of the novel peak observed in the corresponding SEP (**Figure 2C**). As for SS firing, in both genotypes we observed a slight decrease in SS firing probability just after the CS occurrence, between 15-18 ms for WT and 6-10 ms for KO mice, but these differences were not significant. Although the precise origin of this novel peak needs to be elucidated, the data suggest that the cerebellar representation of cortical input is anticipated in *Cntnap2*$^{-/-}$ mice.

Figure 2. Altered cerebellar LFP after electrical stimulation of the whisker pad in *Cntnap2* KOs. (A) Schematic illustration representing the LFP recording. (B) Event-related potential (ERP) analysis comparing the

eNeuro Accepted Manuscript

average SEP traces for 9 KO (red trace) and 6 WT mice (black trace). Vertical pink bars indicate statistically different latencies, corresponding to the cortical peak (C) in WT at 12.87±0.40 ms, which is absent in KOs, who show a statistically significant novel negative peak, presumably an anticipated cortical response, at 6.46±0.14 ms. Student's t-test ($P<0.05$). (C) Temporal firing pattern for SS (left) and CS (right) in WT (N= 6 neurons, black) and KO (N= 10 neurons, red) mice after electrical stimulation. Note that CS appear at post-stimulation latencies concordant with the C component in WT, while they appear earlier in KO mice, likely indicating an anticipated C response at 6 ms. Two-way ANOVA, Holm-Sidak test for multiple comparisons ($P<0.0001$). The graphs represent the mean ± S.E.M (discontinuous or shaded lines).

Increased Purkinje cell intrinsic excitability in *Cntnap2* KO mice

To assess if alterations in the intrinsic properties of PC could be responsible for the aberrant firing found during spontaneous or evoked activity, we performed whole cell patch-clamp recordings of PC from the Crus I/II area in sagittal cerebellar slices. No differences were found in passive membrane properties (resting potential, input resistance, membrane capacitance) between WT and *Cntnap2* KO mice (**Figure 3A**). Similarly, no differences in action potential (AP) threshold were found between genotypes (**Figure 3B**). The injected current needed to evoke the first action potential (rheobase) was smaller in *Cntnap2* KOs (**Figure 3C**), suggesting increased excitability. To specifically study PC intrinsic excitability, we measured the neuronal firing frequency elicited by depolarizing current steps of increasing amplitude. Both genotypes showed a linear current/frequency increase, as described for PC (Llinas and Sugimori, 1980; Fernandez et al., 2007) but, as expected based on their smaller rheobase, PC in *Cntnap2* KO mice fired at a higher frequency for the same injected current, indicating higher excitability (**Figure 3D**). The slopes of the individual current/frequency lines of the neurons for each genotype were also analyzed showing that specifically a subgroup of neurons seem to be driving the observed excitability effects.

Reduced dendritic complexity of Purkinje cells in *Cntnap2* mice

Recently, *Cntnap2* has been reported to modulate the development of PC (Argent et al., 2020). Further, we previously demonstrated that *Cntnap2* KO mice show defects in spine stabilization

eNeuro Accepted Manuscript

in the cerebral cortex (Gdalyahu et al., 2015). To determine whether the electrophysiological alterations observed in PC in *Cntnap2* KOs are associated with morphological changes, we characterized PC morphology in the patched neurons by biocytin staining (**Figure 4A**). We found that the overall length of the cells is significantly smaller in *Cntnap2* mice (**Figure 4B**). Sholl analysis of dendritic complexity demonstrated that PC of KO mice not only are smaller but also have a less complex dendritic arbor (**Figure 4C**). Last, no statistically significant differences in spine density were found between genotypes (**Figure 4D**).

Figure 3. **Increased intrinsic excitability of Purkinje cells in *Cntnap2* KOs.** (A) Representative action potential from WT and KO mice. No significant differences were found in passive membrane properties between WT and KO PC. Resting potential MD 0.6720 [95.0% CI -3.7, 5.15], Student t test P=0.778. Input resistance MD 0.263 [95.0% CI -25.5, 20.1], Student *t* test P=0.986. Capacitance MD -13.22 [95.0% CI -76.5, 46.7], Student *t* test P=0.691 (B) Action potential (AP) threshold MD -2.180 [95.0% CI -8.12, 3.88], Student *t* test P=0.499. (C) Rheobase MD -205 [95.0% CI -382, -36.4], Student t test P=0.034. (D) Intrinsic excitability as a measurement of firing frequency upon current step increases (left) and individual slopes of the frequency/intensity lines (right). Two-way ANOVA mixed effect (interaction genotype x current P=0.03), slopes MD 0.0679 [95.0% CI 0.00631, 0.163], Student *t* test P=0.12. All data are presented as mean ± S.E.M. N= 11WT, 13 KO neurons. MD= mean difference (KO-WT); CI, confidence interval. *P<0.05. Membrane potentials are not corrected for the liquid junction potential between intra and external solution (-12.7 mV).

Figure 4. Reduced arborization of Purkinje cells in *Cntnap2* KOs. (A) Representation of Sholl analysis applied to a PC. (B) PC length from soma to the most apical point, MD -61.89 [95.0% CI -89.6, -35.7], Student's *t* test P=0.0002. N=14 WT, 15KO (C) Number of intersections as a function of their distance from the soma. Two-Way ANOVA with repeated measures. N=11 WT, 16 KO. (D) Spine density MD 0.246 [95.0% CI -0.0533, 0.532], Student's *t* test P=0.117. N= 20 WT, 18 KO. Data are presented as mean ± S.E.M. MD= mean difference (KO-WT); CI, confidence interval. **P<0.01, ***P<0.001.

eNeuro Accepted Manuscript

Discussion

There is growing evidence for the involvement of the cerebellum in ASD through its role in integrating sensory neural signals. In this work, we investigated sensory processing in the cerebellum *in vivo* in the *Cntnap2* mouse model of autism, an autism-linked gene involved in cerebellar development and function. We used a well-characterized paradigm to study cerebellar processing of sensory function, where the evoked activity of PC, the sole output of the cerebellum, is analyzed upon whisker stimulation (Cheron et al., 2013). Whisker-related sensory information is conveyed to the cerebellar area Crus I/II, which has been widely associated with ASD (Fernandez et al., 2019), making it an ideal area of study. We found that the evoked response of PC to sensory stimuli (electrical stimulation of the whisker pad) was strikingly different between WT and *Cntnap2* KO mice, as denoted by the generated SEP. Whisker information reaches the cerebellum via two routes, the pontine nuclei-parallel fiber pathway and the inferior olive-climbing fiber pathway (Kleinfeld et al., 1999), generating the two distinct types of firing that characterize PC: SS and CS, respectively. Individual analysis of each type of spike upon stimulation revealed that the timing of appearance of the stimulus-evoked CS, anticipated in *Cntnap2* KOs, was driving the observed differences in SEP, indicating an altered processing of climbing fiber inputs. In agreement with this, dysfunction of the olivocerebellar circuit in *Cntnap2* mice was proposed as responsible for the decreased response probability shown by this model in the eye-blink conditioning test, another paradigm widely used to study cerebellar function (Kloth et al., 2015). The appearance of the stimulus-evoked CS has been shown to be modulated by activity from the somatosensory cortex, since the suppression of S1 activity abolishes CS appearance upon tactile stimulation (Shimuta et al., 2020). Further, diminishing S1 activity lengthens and enhancing it shortens CS appearance latency (Brown and Bower, 2002). These data would suggest that increased activity of S1 could be responsible for the observed CS anticipation in the *Cntnap2* model. In fact, decreased inhibitory markers and increased excitation/inhibition ratio leading to higher cortical sensory gain have been described in *Cntnap2* mice (Penagarikano et al., 2011; Antoine et al., 2019), which could account for the observed deficits.

CS have been recently shown to control the information encoded by SS activity (Streng et al., 2017) in a way that a dynamic relationship between CS and SS is necessary for the initiation of

eNeuro Accepted Manuscript

sensory-driven behavior (Tsutsumi et al., 2020). We observed reduced spontaneous CS firing frequency as well as increased irregularity in the SS timing, despite normal SS firing frequency. The rhythmicity of PC inter-spike intervals is thought to affect the transmission of information to downstream neurons. It is worth noting that increased coefficient of variation has been reported in other animal models of autism with cerebellar dysfunction including *CACNA1A* (Damaj et al., 2015; Jayabal et al., 2016), *CAMK2B* (van Woerden et al., 2009; Kury et al., 2017) and *KCNMA1* (Laumonnier et al., 2006; Chen et al., 2010), being the last two also associated with a reduced CS firing frequency. In the adult stage, each PC receives strong excitatory inputs through a single climbing fiber from the inferior olive, which innervates several PCs, generating CS activity. As CNTNAP2 has been shown to be expressed not only in PCs, but also in inferior olivary neurons (Kloth et al., 2015), alterations in these neurons could likely change the baseline firing rate of CS and could in turn affect the regularity of SS.

Given the observed spontaneous PC firing in vivo, the observation of increased PC excitability and reduced arborization in *Cntnap2* KOs was unexpected. It must be noted that normal PC arborization was described for this same model (Kloth et al., 2015). One possible explanation for this discrepancy is methodological differences (Golgi stain vs. neuronal filling) or more likely a different cerebellar area was analyzed. In fact, it has been recently shown that the cerebellar cortex is non-uniform and that several features of PCs, including activity levels and dendritic arborization develop differentially based on the specific cerebellar area where they are located (Beekhof et al., 2021). On the other hand, voltage-gated potassium (Kv) channels, such as Kv3.3, has been involved in regulating CS. CNTNAP2 is known to cluster Kv channels, including KCNA1 (Kv1.1), KCNA2 (Kv1.2) (Poliak et al., 1999). Reduced expression of such channels was observed in hippocampal tissue resected from epileptic patients harboring *CNTNAP2* mutations (Strauss et al., 2006). Whether the observed alterations in PC excitability are due to reduced expression or mislocalization of Kv channels and its contribution to circuit dysfunction remains to be investigated.

In summary, we report an altered cerebellar response to evoked sensory stimuli in alert *Cntnap2* mice. This alteration is found in conjuction with neuroanatomical and electrophysiological dysfunction of PC. This mouse model, therefore, provides a valuable tool to study the basis for the altered processing of sensory information observed in ASD.

eNeuro Accepted Manuscript

Acknowledgments

The authors thank the SGIker Microscopy Core (UPV/EHU, ERDF, ESF) for technical support and Drs. Jorge Valero and Jan Tønnesen, from Achucarro Basque Center for Neuroscience, for help with neuroanatomical analyses. This work was supported by MCIU/AEI/FEDER, UE grant RTI2018-101427-B-I00 to OP, ERANET-NEURON grant nEUrotalk to OP and UPV/EHU grant GIU18/094 to OP; Israel Science Foundation (536/19) to SK; Spanish Ministry of Science (Europa Excelencia 15/02, SAF2016-78071-R to SK; BFU2017-89615-P from the Spanish MINECO-FEDER to JMR. MF holds a MINECO predoctoral fellowship (BES-2016-078420) and TS-A is a Basque Government predoctoral fellow (PRE-2020-2-0109).

Competing interests

The authors declare no competing interests.

References

Antoine MW, Langberg T, Schnepel P, Feldman DE (2019) Increased Excitation-Inhibition Ratio Stabilizes Synapse and Circuit Excitability in Four Autism Mouse Models. Neuron 101:648-661 e644.https://www.ncbi.nlm.nih.gov/pubmed/30679017

APA (2013) Diagnostic and Statistical Manual of Mental Disorders, 5th Edition: DSM-5. American Psychiatric Association

Argent L, Winter F, Prickett I, Carrasquero-Ordaz M, Olsen AL, Kramer H, Lancaster E, Becker EBE (2020) Caspr2 interacts with type 1 inositol 1,4,5-trisphosphate receptor in the developing cerebellum and regulates Purkinje cell morphology. J Biol Chem 295:12716-12726.https://www.ncbi.nlm.nih.gov/pubmed/32675284

Becker EB, Zuliani L, Pettingill R, Lang B, Waters P, Dulneva A, Sobott F, Wardle M, Graus F, Bataller L, Robertson NP, Vincent A (2012) Contactin-associated protein-2 antibodies in non-paraneoplastic cerebellar ataxia. J Neurol Neurosurg Psychiatry 83:437-440.https://www.ncbi.nlm.nih.gov/pubmed/22338029

Beekhof GC, Osorio C, White JJ, van Zoomeren S, van der Stok H, Xiong B, Nettersheim IH, Mak WA, Runge M, Fiocchi FR, Boele HJ, Hoebeek FE, Schonewille M (2021) Differential spatiotemporal development of Purkinje cell populations and cerebellum-dependent sensorimotor behaviors. Elife 10.https://www.ncbi.nlm.nih.gov/pubmed/33973524

Brown IE, Bower JM (2002) The influence of somatosensory cortex on climbing fiber responses in the lateral hemispheres of the rat cerebellum after peripheral tactile stimulation. J Neurosci 22:6819-6829.https://www.ncbi.nlm.nih.gov/pubmed/12151562

eNeuro Accepted Manuscript

Chen X, Kovalchuk Y, Adelsberger H, Henning HA, Sausbier M, Wietzorrek G, Ruth P, Yarom Y, Konnerth A (2010) Disruption of the olivo-cerebellar circuit by Purkinje neuron-specific ablation of BK channels. Proc Natl Acad Sci U S A 107:12323-12328.https://www.ncbi.nlm.nih.gov/pubmed/20566869

Cheron G, Dan B, Marquez-Ruiz J (2013) Translational approach to behavioral learning: lessons from cerebellar plasticity. Neural Plast 2013:853654.https://www.ncbi.nlm.nih.gov/pubmed/24319600

D'Mello AM, Moore DM, Crocetti D, Mostofsky SH, Stoodley CJ (2016) Cerebellar gray matter differentiates children with early language delay in autism. Autism Res 9:1191-1204.https://www.ncbi.nlm.nih.gov/pubmed/27868392

Damaj L, Lupien-Meilleur A, Lortie A, Riou E, Ospina LH, Gagnon L, Vanasse C, Rossignol E (2015) CACNA1A haploinsufficiency causes cognitive impairment, autism and epileptic encephalopathy with mild cerebellar symptoms. Eur J Hum Genet 23:1505-1512.https://www.ncbi.nlm.nih.gov/pubmed/25735478

Dawes JM et al. (2018) Immune or Genetic-Mediated Disruption of CASPR2 Causes Pain Hypersensitivity Due to Enhanced Primary Afferent Excitability. Neuron 97:806-822 e810.https://www.ncbi.nlm.nih.gov/pubmed/29429934

Ellegood J, Crawley JN (2015) Behavioral and Neuroanatomical Phenotypes in Mouse Models of Autism. Neurotherapeutics 12:521-533.https://www.ncbi.nlm.nih.gov/pubmed/26036957

Fernandez FR, Engbers JD, Turner RW (2007) Firing dynamics of cerebellar purkinje cells. J Neurophysiol 98:278-294.https://www.ncbi.nlm.nih.gov/pubmed/17493923

Fernandez M, Sierra-Arregui T, Penagarikano O (2019) Thew cerebellum and autism, more than motor control. In: Behavioral Neuroscience. London, UK: IntechOpen.

Gao JH, Parsons LM, Bower JM, Xiong J, Li J, Fox PT (1996) Cerebellum implicated in sensory acquisition and discrimination rather than motor control. Science 272:545-547.https://www.ncbi.nlm.nih.gov/pubmed/8614803

Gdalyahu A, Lazaro M, Penagarikano O, Golshani P, Trachtenberg JT, Geschwind DH (2015) The Autism Related Protein Contactin-Associated Protein-Like 2 (CNTNAP2) Stabilizes New Spines: An In Vivo Mouse Study. PLoS One 10:e0125633.https://www.ncbi.nlm.nih.gov/pubmed/25951243

Gordon A, Salomon D, Barak N, Pen Y, Tsoory M, Kimchi T, Peles E (2016) Expression of Cntnap2 (Caspr2) in multiple levels of sensory systems. Mol Cell Neurosci 70:42-53.https://www.ncbi.nlm.nih.gov/pubmed/26647347

Holt GR, Softky WR, Koch C, Douglas RJ (1996) Comparison of discharge variability in vitro and in vivo in cat visual cortex neurons. J Neurophysiol 75:1806-1814.https://www.ncbi.nlm.nih.gov/pubmed/8734581

Jayabal S, Chang HH, Cullen KE, Watt AJ (2016) 4-aminopyridine reverses ataxia and cerebellar firing deficiency in a mouse model of spinocerebellar ataxia type 6. Sci Rep 6:29489.https://www.ncbi.nlm.nih.gov/pubmed/27381005

Kleinfeld D, Berg RW, O'Connor SM (1999) Anatomical loops and their electrical dynamics in relation to whisking by rat. Somatosens Mot Res 16:69-88.https://www.ncbi.nlm.nih.gov/pubmed/10449057

Kloth AD, Badura A, Li A, Cherskov A, Connolly SG, Giovannucci A, Bangash MA, Grasselli G, Penagarikano O, Piochon C, Tsai PT, Geschwind DH, Hansel C, Sahin M, Takumi T,

eNeuro Accepted Manuscript

Worley PF, Wang SS (2015) Cerebellar associative sensory learning defects in five mouse autism models. Elife 4:e06085.https://www.ncbi.nlm.nih.gov/pubmed/26158416

Kury S et al. (2017) De Novo Mutations in Protein Kinase Genes CAMK2A and CAMK2B Cause Intellectual Disability. Am J Hum Genet 101:768-788.https://www.ncbi.nlm.nih.gov/pubmed/29100089

Laumonnier F, Roger S, Guerin P, Molinari F, M'Rad R, Cahard D, Belhadj A, Halayem M, Persico AM, Elia M, Romano V, Holbert S, Andres C, Chaabouni H, Colleaux L, Constant J, Le Guennec JY, Briault S (2006) Association of a functional deficit of the BKCa channel, a synaptic regulator of neuronal excitability, with autism and mental retardation. Am J Psychiatry 163:1622-1629.https://www.ncbi.nlm.nih.gov/pubmed/16946189

Lidstone DE, Rochowiak R, Mostofsky SH, Nebel MB (2021) A Data Driven Approach Reveals That Anomalous Motor System Connectivity is Associated With the Severity of Core Autism Symptoms. Autism Res.https://www.ncbi.nlm.nih.gov/pubmed/33484109

Llinas R, Sugimori M (1980) Electrophysiological properties of in vitro Purkinje cell somata in mammalian cerebellar slices. J Physiol 305:171-195.https://www.ncbi.nlm.nih.gov/pubmed/7441552

Marquez-Ruiz J, Cheron G (2012) Sensory stimulation-dependent plasticity in the cerebellar cortex of alert mice. PLoS One 7:e36184.https://www.ncbi.nlm.nih.gov/pubmed/22563448

Melzer N, Golombeck KS, Gross CC, Meuth SG, Wiendl H (2012) Cytotoxic CD8+ T cells and CD138+ plasma cells prevail in cerebrospinal fluid in non-paraneoplastic cerebellar ataxia with contactin-associated protein-2 antibodies. J Neuroinflammation 9:160.https://www.ncbi.nlm.nih.gov/pubmed/22759321

Mostofi A, Holtzman T, Grout AS, Yeo CH, Edgley SA (2010) Electrophysiological localization of eyeblink-related microzones in rabbit cerebellar cortex. J Neurosci 30:8920-8934.https://www.ncbi.nlm.nih.gov/pubmed/20592214

Penagarikano O, Abrahams BS, Herman EI, Winden KD, Gdalyahu A, Dong H, Sonnenblick LI, Gruver R, Almajano J, Bragin A, Golshani P, Trachtenberg JT, Peles E, Geschwind DH (2011) Absence of CNTNAP2 leads to epilepsy, neuronal migration abnormalities, and core autism-related deficits. Cell 147:235-246.https://www.ncbi.nlm.nih.gov/pubmed/21962519

Poliak S, Gollan L, Martinez R, Custer A, Einheber S, Salzer JL, Trimmer JS, Shrager P, Peles E (1999) Caspr2, a new member of the neurexin superfamily, is localized at the juxtaparanodes of myelinated axons and associates with K+ channels. Neuron 24:1037-1047.https://www.ncbi.nlm.nih.gov/pubmed/10624965

Proville RD, Spolidoro M, Guyon N, Dugue GP, Selimi F, Isope P, Popa D, Lena C (2014) Cerebellum involvement in cortical sensorimotor circuits for the control of voluntary movements. Nat Neurosci 17:1233-1239.https://www.ncbi.nlm.nih.gov/pubmed/25064850

Rodenas-Cuadrado P, Pietrafusa N, Francavilla T, La Neve A, Striano P, Vernes SC (2016) Characterisation of CASPR2 deficiency disorder--a syndrome involving autism, epilepsy and language impairment. BMC Med Genet 17:8.https://www.ncbi.nlm.nih.gov/pubmed/26843181

Sanchez-Leon CA, Cordones I, Ammann C, Ausin JM, Gomez-Climent MA, Carretero-Guillen A, Sanchez-Garrido Campos G, Gruart A, Delgado-Garcia JM, Cheron G, Medina JF,

eNeuro Accepted Manuscript

Marquez-Ruiz J (2021) Immediate and after effects of transcranial direct-current stimulation in the mouse primary somatosensory cortex. Sci Rep 11:3123.https://www.ncbi.nlm.nih.gov/pubmed/33542338

Scott KE, Schormans AL, Pacoli KY, De Oliveira C, Allman BL, Schmid S (2018) Altered Auditory Processing, Filtering, and Reactivity in the Cntnap2 Knock-Out Rat Model for Neurodevelopmental Disorders. J Neurosci 38:8588-8604.https://www.ncbi.nlm.nih.gov/pubmed/30126973

Shimuta M, Sugihara I, Ishikawa T (2020) Multiple signals evoked by unisensory stimulation converge onto cerebellar granule and Purkinje cells in mice. Commun Biol 3:381.https://www.ncbi.nlm.nih.gov/pubmed/32669638

Skefos J, Cummings C, Enzer K, Holiday J, Weed K, Levy E, Yuce T, Kemper T, Bauman M (2014) Regional alterations in purkinje cell density in patients with autism. PLoS One 9:e81255.https://www.ncbi.nlm.nih.gov/pubmed/24586223

Strauss KA, Puffenberger EG, Huentelman MJ, Gottlieb S, Dobrin SE, Parod JM, Stephan DA, Morton DH (2006) Recessive symptomatic focal epilepsy and mutant contactin-associated protein-like 2. N Engl J Med 354:1370-1377.https://www.ncbi.nlm.nih.gov/pubmed/16571880

Streng ML, Popa LS, Ebner TJ (2017) Climbing Fibers Control Purkinje Cell Representations of Behavior. J Neurosci 37:1997-2009.https://www.ncbi.nlm.nih.gov/pubmed/28077726

Tan GC, Doke TF, Ashburner J, Wood NW, Frackowiak RS (2010) Normal variation in fronto-occipital circuitry and cerebellar structure with an autism-associated polymorphism of CNTNAP2. Neuroimage 53:1030-1042.https://www.ncbi.nlm.nih.gov/pubmed/20176116

Tang T, Xiao J, Suh CY, Burroughs A, Cerminara NL, Jia L, Marshall SP, Wise AK, Apps R, Sugihara I, Lang EJ (2017) Heterogeneity of Purkinje cell simple spike-complex spike interactions: zebrin- and non-zebrin-related variations. J Physiol 595:5341-5357.https://www.ncbi.nlm.nih.gov/pubmed/28516455

Tsutsumi S, Chadney O, Yiu TL, Baumler E, Faraggiana L, Beau M, Hausser M (2020) Purkinje Cell Activity Determines the Timing of Sensory-Evoked Motor Initiation. Cell Rep 33:108537.https://www.ncbi.nlm.nih.gov/pubmed/33357441

van Woerden GM, Hoebeek FE, Gao Z, Nagaraja RY, Hoogenraad CC, Kushner SA, Hansel C, De Zeeuw CI, Elgersma Y (2009) betaCaMKII controls the direction of plasticity at parallel fiber-Purkinje cell synapses. Nat Neurosci 12:823-825.https://www.ncbi.nlm.nih.gov/pubmed/19503086

Wang SS, Kloth AD, Badura A (2014) The cerebellum, sensitive periods, and autism. Neuron 83:518-532.https://www.ncbi.nlm.nih.gov/pubmed/25102558

Wang Y, Xu Q, Zuo C, Zhao L, Hao L (2020) Longitudinal Changes of Cerebellar Thickness in Autism Spectrum Disorder. Neurosci Lett 728:134949.https://www.ncbi.nlm.nih.gov/pubmed/32278028

eNeuro Accepted Manuscript

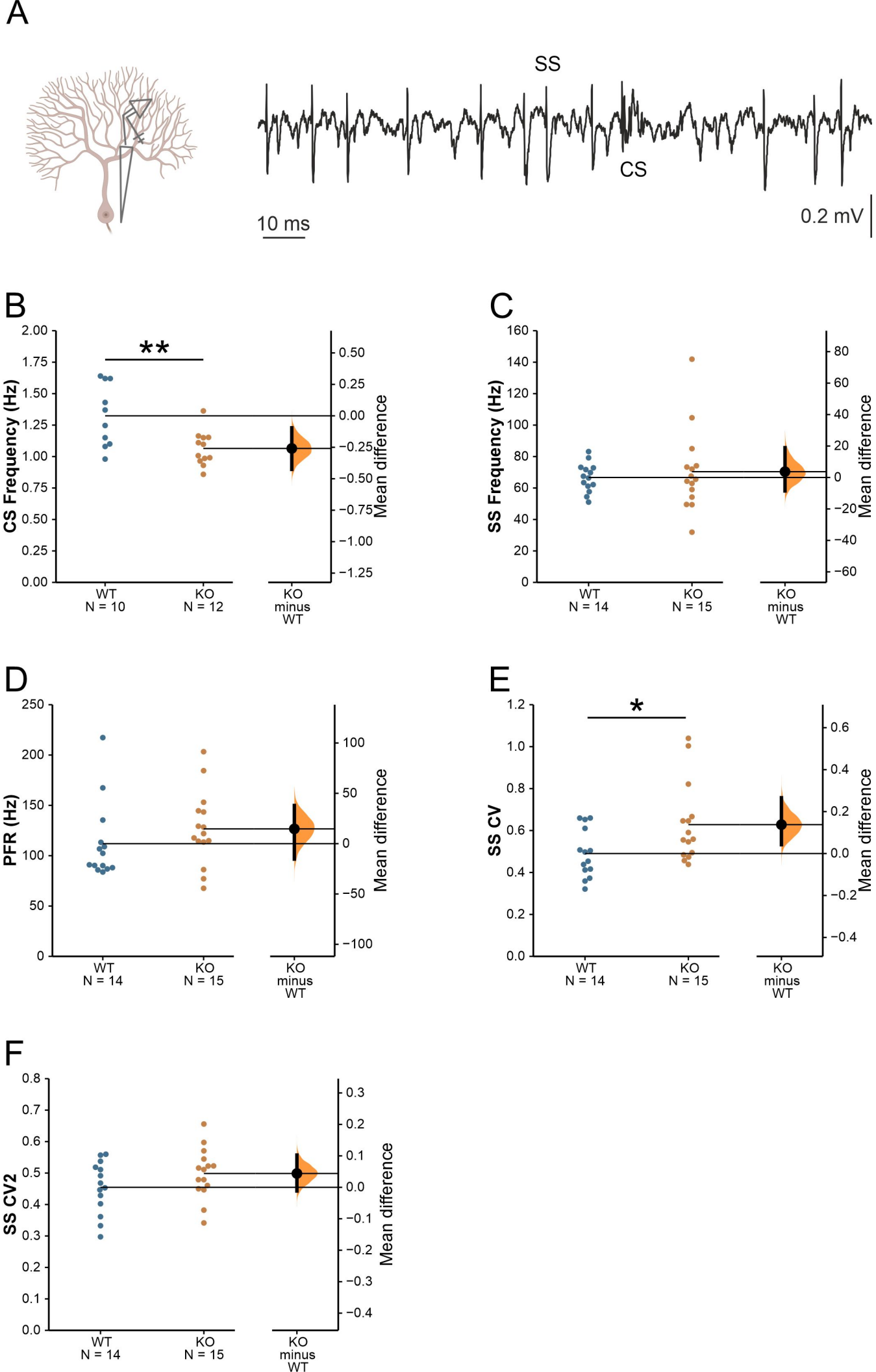

eNeuro Accepted Manuscript

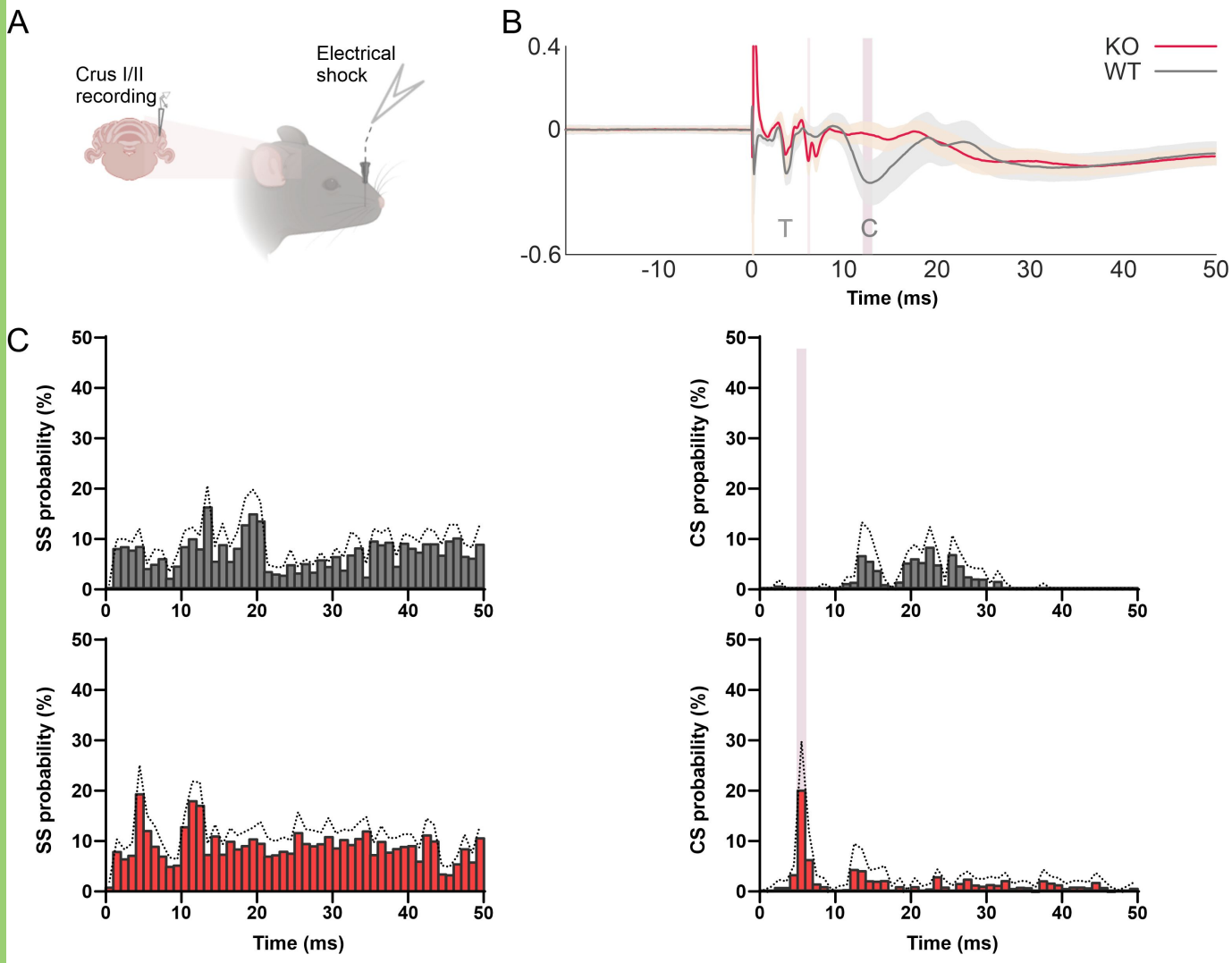

eNeuro Accepted Manuscript

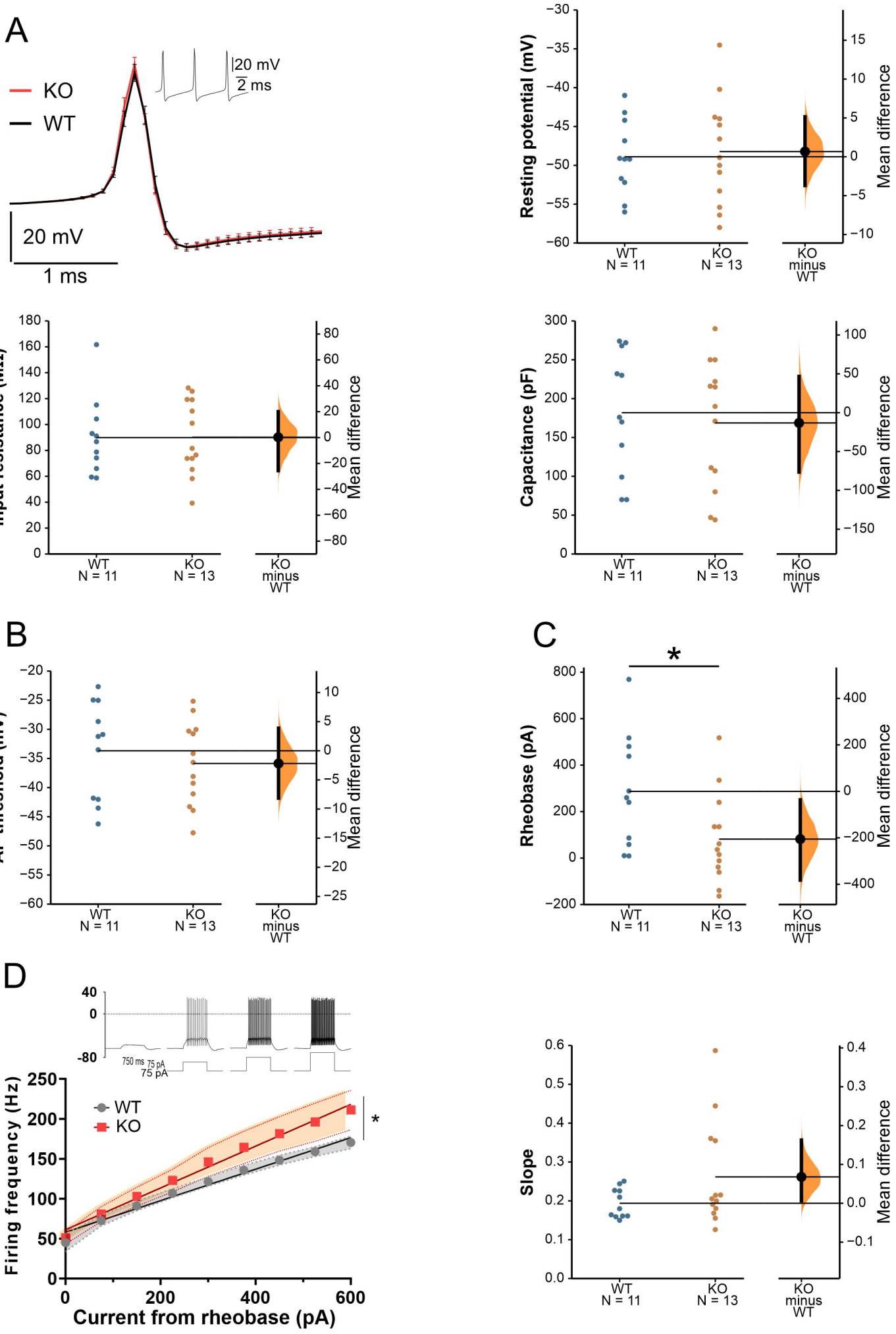

eNeuro Accepted Manuscript